Accepted Manuscript

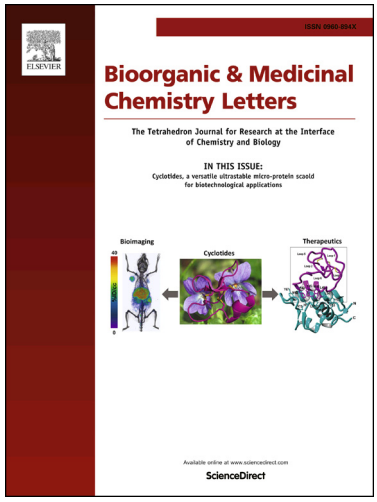

In-vitro and *In-silico* evaluations of diarylpentanoid series as α-glucosidase inhibitor

Sze Wei Leong, Faridah Abas, Lam Kok Wai, Khatijah Yusoff

PII: S0960-894X(17)31222-2
DOI: https://doi.org/10.1016/j.bmcl.2017.12.048
Reference: BMCL 25504

To appear in: *Bioorganic & Medicinal Chemistry Letters*

Received Date: 19 September 2017
Revised Date: 7 December 2017
Accepted Date: 21 December 2017

Please cite this article as: Wei Leong, S., Abas, F., Kok Wai, L., Yusoff, K., *In-vitro* and *In-silico* evaluations of diarylpentanoid series as α-glucosidase inhibitor, *Bioorganic & Medicinal Chemistry Letters* (2017), doi: https://doi.org/10.1016/j.bmcl.2017.12.048

Graphical Abstract

To create your abstract, type over the instructions in the template box below.
Fonts or abstract dimensions should not be changed or altered.

IN-VITRO AND _IN-SILICO_ EVALUATIONS OF DIARYLPENTANOID SERIES AS α-GLUCOSIDASE INHIBITOR

Leave this area blank for abstract info.

Sze Wei Leong[a,b], Faridah Abas,[b,c*], Lam Kok Wai[d], Khatijah Yusoff[a]

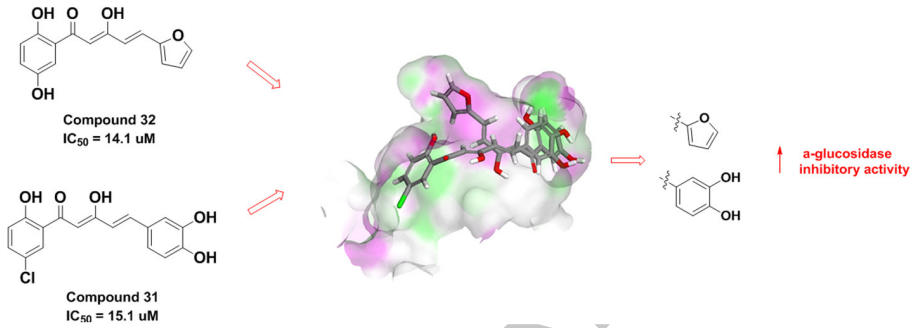

ELSEVIER

Bioorganic & Medicinal Chemistry Letters
journal homepage: www.elsevier.com

In-vitro and *In-silico* evaluations of diarylpentanoid series as α-glucosidase inhibitor

Sze Wei Leong[a,b], Faridah Abas[b,c*], Lam Kok Wai[d], Khatijah Yusoff[a]

[a]*Department of Microbiology, Faculty of Biotechnology and Biomolecular Sciences, Universiti Putra Malaysia, 43400 UPM, Serdang, Selangor, Malaysia.*
[b]*Laboratory of Natural Products, Institute of Bioscience, Universiti Putra Malaysia, 43400 UPM, Serdang, Selangor, Malaysia.*
[c]*Department of Food Science, Faculty of Food Science and Technology, Universiti Putra Malaysia, 43400 UPM, Serdang, Selangor, Malaysia.*
[d]*Drug and Herbal Research Centre Faculty of Pharmacy, Universiti Kebangsaan Malaysia, Jalan Raja Muda Abd. Aziz, 50300 Kuala Lumpur, Malaysia.*

ARTICLE INFO

Article history:
Received
Received in revised form
Accepted
Available online

Keywords:
Diarylpentanoids
α-Glucosidase inhibitory activity
Docking
Polyhydroxyphenyl
Furanyl

ABSTRACT

A series of thirty-four diarylpentanoids derivatives were synthesized and evaluated for their α-glucosidase inhibitory activity. Eleven compounds (**19, 20, 21, 24, 27, 28, 29, 31, 32, 33** and **34**) were found to significantly inhibit α-glucosidase in which compounds **28, 31** and **32** demonstrated the highest activity with IC_{50} values ranging from 14.1 to 15.1 μM. Structure-activity comparison shows that multiple hydroxy groups are essential for α-glucosidase inhibitory activity. Meanwhile, 3,4-dihydroxyphenyl and furanyl moieties were found to be crucial in improving α-glucosidase inhibition. Molecular docking analyses further confirmed the critical role of both 3,4-dihydroxyphenyl and furanyl moieties as they bound to α-glucosidase active site in different mode. Overall result suggests that diarylpentanoids with both five membered heterocyclic ring and polyhydroxypheny moiety could be a new lead design in the search of novel α-glucosidase inhibitor.

Diabetes Mellitus (DM) is a prevalent metabolic disorder characterized by prolonged fasting hyperglycemia resulted from inadequate production (type 1) or inefficient utilization (type 2) of insulin.[1] The unattended chronic hyperglycemia could narrow, block or even damage the body's blood vessels and eventually lead to serious complications such as heart attack, stroke, kidney failure, leg amputation, vision loss and nerve damage.[2-7] According to Global Report on Diabetes released by World Health Organization (WHO) in 2016, DM has affected more than 422 million adults globally and the number is expected to rise beyond 592 million in 2035.[8] On top of this, DM has caused 4.9 million of deaths and at least USD 612 billion of annual global health expenditure in 2014.[9] Thus, by considering global health and economics impacts, cheaper and safer treatments for DM must be pursued urgently and unremittingly.

Recently, α-glucosidase has been recognized as a therapeutic target for treating type-2 DM based upon its pivotal role in carbohydrates digestion. α-Glucosidase is a membrane-bound intestinal enzyme found in small intestine epithelium which responsible for the hydrolysis of carbohydrates to monosaccharides such as glucose. The converted glucose will then absorbed into blood stream resulting in increased blood glucose level.[10-12] Thus, inhibiting α-glucosidase may reduce postprandial hyperglycemia by delaying glucose conversion and absorption. Several α-glucosidase inhibitors such as acarbose, miglitol and voglibose have been widely used in treating type-2 diabetes. However, various side effects including bloating, flatulence and diarrhea were encountered throughout the treatments.[10, 13, 14] On account of this, new safer α-glucosidase inhibitors with minimal side effects are urgently warranted.

Diarylpentanoids is the most potent family of curcuminoid derivatives due to its excellent stability and multiple medicinal properties. Diarylpentanoids are well-known for their great antioxidant and anti-inflammatory properties based upon their ability in suppressing numerous free radicals and pro-inflammatory cytokines such as 2,2-diphenyl-1-picrylhydrazyl (DPPH) free radical, superoxide radical, hydroxyl radical, tumor necrosis factor alpha (TNF-a), and interleukins.[15-17] On top of this, diarylpentanoids were also recognized as potent anti-cancer agents by their outstanding inhibition on various cancer cell lines as well as *in-vivo* tumor suppression effects on both zebra fish and BALB/c nude mouse models.[18-23] Interestingly, recent studies reported that diarylpentanoids are non-toxic on *in-vivo* mice models which provide them with extra tokens in the search of new drug with minimal side effects.[24, 25]

Previously we have reported several series of diarylpentanoids with improved stability as well as antioxidant, anti-inflammatory and anti-Alzheimer's properties.[26-30] In continuing our efforts in exploring the pharmacological potential of diarylpentanoids, we further derivatize and investigate their inhibitory effects on α-glucosidase.

Scheme 1. General synthetic steps for compounds **1-21**[x]

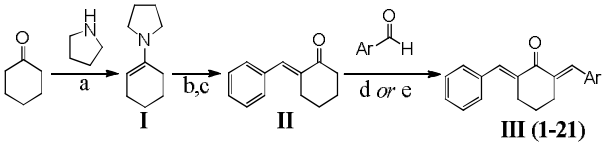

[x]Reagents and conditions: (a) *p*-toluene-sulphonic acid, toluene, reflux (2h); (b) benzaldehyde, 80°C (8 h); (c) H_2O, reflux (0.5h); (d) NaOH, EtOH, RT (overnight); (e) benzaldehyde, acetic acid, H_2SO_4, RT (overnight).

As shown in Scheme 1, compounds **1-21** (**III**) were achieved through enamine-catalyzed benzylidenation followed by NaOH- or H_2SO_4-catalyzed Claisen-Schmidt condensations.[31] Accordingly, cyclohexanone is first reacted with pyrrolidine to form N-(1-cyclohexenyl)pyrrolidine (**I**) in a Dean-Stark reflux setup. The reaction progress was determined by measuring the amount of H_2O collected in the Dean-Stark burette collector. Upon the completion, the enamine **I** crude was further reacted with benzaldehyde at 80°C followed by hydrolysis with water to afford the targeted intermediate **II**, 2-benzylidenecyclohexanone. The purified pale yellow intermediate **II** was finally reacted with appropriate aryl aldehydes to achieve the desired compounds **III** (**1-21**). In this step, H_2SO_4 was used to catalyze the reaction with hydroxylated benzaldehyde while non-hydroxylated benzaldehydes was reacted in NaOH condition.

All synthesized compounds were purified by flash chromatography and characterized by ^{1}H-NMR, ^{13}C-NMR, and high-resolution electron ionization-mass spectrometry. The purified compounds used for α-glucosidase inhibitory evaluations were of 95 to 99% purity based on their respective HPLC profiles. All purified compounds were screened for their α-glucosidase inhibitory activity at 50 µM test concentration and the screening result is depicted in **Figure 1**.[32]

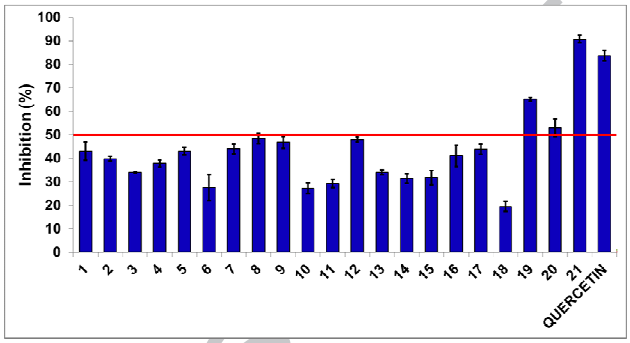

Figure 1. α-Glucosidase inhibitory effects of compounds **1–21** at a testing concentration of 50 µM

As illustrated in Figure 1, there are three compounds successfully suppressed α-glucosidase activity with the percentage of inhibition greater than 50%. The three active compounds were then subjected to IC_{50} determination and the values obtained were compared to that of the positive control, quercetin. The overall α-glucosidase inhibitory effect of twenty-five analogs is tabulated in **Table 1**.

Table 1. α-Glucosidase suppression of compounds **1-21**.

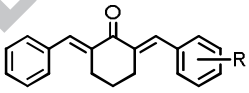

Compounds	R	Inhibition % at 50 µM	IC_{50} (µM)	Compounds	R	Inhibition % at 50 µM	IC_{50} (µM)
1	2-F	43.0	ND	**12**	3-CH_3	47.9	ND
2	3-F	39.8	ND	**13**	4-CH_3	34.1	ND
3	4-F	34.0	ND	**14**	4-OME	31.4	ND
4	3,4-F	37.8	ND	**15**	2,3-OME	31.8	ND
5	2-Cl	43.0	ND	**16**	2,4-OME	41.0	ND
6	4-Cl	27.6	ND	**17**	2,5-OME	43.8	ND
7	2,3-Cl	44.0	ND	**18**	3,4,5-OME	16.3	ND
8	3,4-Cl	48.4	ND	**19**	3-OH	65.1	28.4
9	2-Br	46.8	ND	**20**	4-OH	53.0	42.3
10	3-Br	27.2	ND	**21**	3,4-OH	90.7	20.3
11	4-Br	29.1	ND	**QUERCETIN**	-	83.6	7.8

ND = Not determine

As displayed in **Table 1**, compound **21** was found to exhibit strongest α-glucosidase inhibitory effect with the IC_{50} value of 20.3 µM. Meanwhile, compounds **19** and **20** possessed relatively weak activities, giving IC_{50} values of 28.4 and 42.3 µM, respectively. This observation suggesting that hydroxyl moiety is essential for activity as compounds **19-21** are the only hydroxylated analogs. With respect to the substitution pattern of hydroxyl group, *meta*-substitution is preferable since compound **19** exhibited approximately 1.5-fold higher inhibition than its respective *para*-hydroxylated analog **20**. On top of this, polyhydroxy moiety was found to be critical in improving α-glucosidase inhibition of diarylpentanoids as compound **21**, a dihydroxylated analog demonstrated the highest activity. Although none of our analogs shows comparable activity to quercetin, however, in continuing our efforts in identifying α-glucosidase inhibitor based on diarylpentanoid scaffold, we further tested our previously designed hydroxylated compounds (**22-34**) for their α-glucosidase inhibitory activity. **Scheme 2** and **Scheme 3** represent the synthetic steps of compounds **22-24** and **25-34**, respectively.

Scheme 2. General synthetic steps for compounds **22-24**[y]

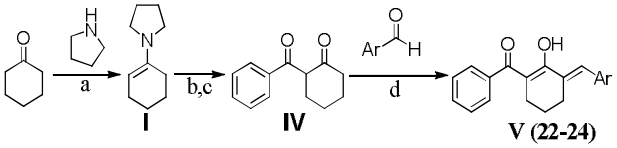

[y]Reagents and conditions: (a) *p*-toluene-sulphonic acid, toluene, reflux (2h); (b) benzoic anhydride, RT (24h); (c) H_2O, reflux (0.5h); (d) hydoxylated benzaldehyde, acetic acid, H_2SO_4, RT (overnight).

Scheme 3. General synthetic steps for compounds **25-34**[z]

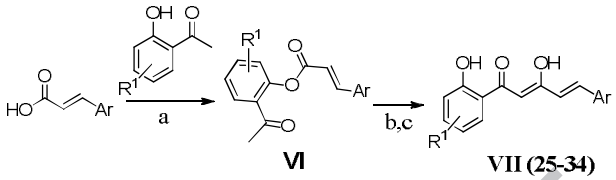

[z]Reagents and conditions: (a) $POCl_3$, pyridine, RT (overnight); (b) KOH, pyridine, RT (overnight); (c) BBr_3, CH_2Cl_2, 0 °C (8 h).

Similar to the synthesis of compounds **1-21**, **22-24** were achieved by Stork enamine acylation and Claisen-Schmidt condensation.[33] As presented in **Scheme 2**, enamine intermediate was first prepared by reacting cycloxanone with pyrrolidine in the presence of *p*-toluene-sulphonic acid. Then, the acylation with benzoic anhydride was carried out to afford 2-benzoylcyclohexanone, **IV.** The purify **IV** was further reacted with hydroxylated benzaldehydes in acid-catalyzed Claisen-Schmidt condensation to yield compounds **22-24**. In preparing compounds **25-34** (**Scheme 3**), different substituted cinnamic acids were first reacted with 2-hydroxyacetophenone analogs to afford colourless cinnamate intermediate, **VI**. Then, the purified **VI** analogs were introduced to Baker-Venkataraman Rearrangement with KOH in pyridine in order to achieve yellow methoxylated diarylpentanoids. Finally, the methoxylated diarylpentanoids were undergone demethylation with BBR_3 in dichloromethane to give polyphenolic diarylpentanoid analogs, compounds **25-34.**[34] All purified compounds were characterized by ^{1}H-NMR, ^{13}C-NMR, and high-resolution electron ionization-mass spectrometry. The purified compounds used for α-glucosidase inhibitory evaluations were of 95 to 99% purity based on their respective HPLC profiles. The overall α-glucosidase inhibitory effects of compounds **22-34** are summarized in **Table 2.**

Table 2. α-Glucosidase suppression of compounds **22-34**.

Compounds	Structure	Inhibition % at 50 µM	IC_{50} (µM)	Compound	Structure	Inhibition % at 50 µM	IC_{50} (µM)
22	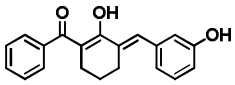	43.2	ND	**29**	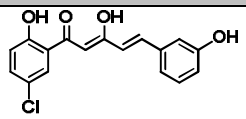	62.4	36.4
23	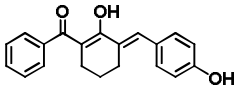	34.9	ND	**30**	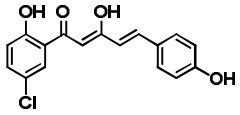	45.3	ND
24	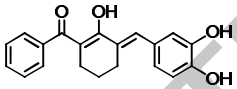	55.9	41.0	**31**	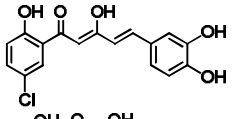	85.6	15.1
25	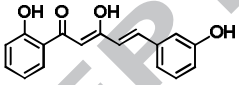	40.4	ND	**32**	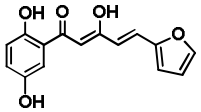	98.4	14.1
26	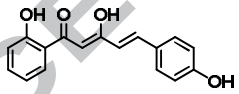	20.4	ND	**33**	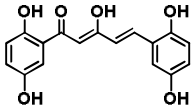	96.9	19.6
27	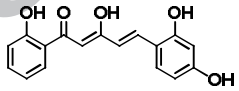	61.2	40.7	**34**	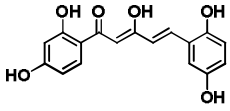	86.6	20.0
28	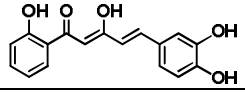	93.6	14.3				

ND = Not determine

According to **Table 2**, the *meta*-substitution of diarylpentanoids continued demonstrates its importance in α-glucosidase inhibition as compounds **22**, **25** and **29** exhibited better activity than compounds **23**, **26** and **30**, respectively. In addition, multiple substitutions of hydroxyl groups on phenyl ring remained to be crucial with regards to α-glucosidase inhibition as polyhydroxylated compounds such as **28, 31, 33** and **34** exhibited highest activities. These findings further confirmed the enhancing effect of *meta*-substitution and critical role of polyhydroxyl moiety in α-glucosidase inhibitory activity. Among polyhydroxylated compounds, 3,4-dihydroxy moiety was found to be the most potent substitution pattern as compounds **28** and **31** are better α-glucosidase inhibitor as compared to compounds **33** and **34**. Surprisingly, the replacement of 2,5-dihydroxy moiety (**33**) with a furanyl ring (**32**) tends to enhance the inhibitory

activity which suggests that furan ring may bind α-glucosidase in a different mode compared with hydroxylated phenyl moieties.

In order to gain functional and structural insights into the binding mode of polyhydroxylated (**31**) and furanylated (**32**) analogs in α-glucosidase, molecular docking was performed using Discovery Studio 3.1.[35] Compound **31** was selected over compound **28** based on its better similarity in structural geometry with respect to compound **32**. Since the crystal structure of *Saccharomyces cerevisiae* α-glucosidase is still not available, a homology model of α-glucosidase was built according to a previously reported method for the molecular docking analysis. Isomaltase (PDB ID: 3A4A) from baker's yeast was chosen as the template for the respective homology model since it shared 71% identity and 84% similarity with *Saccharomyces cerevisiae* α-glucosidase (UniProt ID: P53341). The homologous protein was generated by MODELER protocol and the optimized structure was further validated by Ramachandran plot (**Figure 2**) obtained from RAMPAGE server.[36]

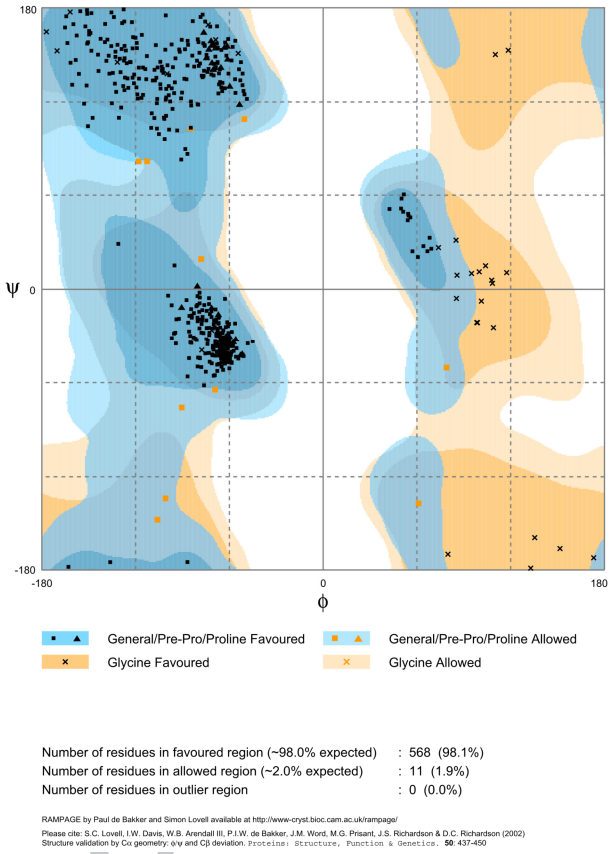

Figure 2. Ramachandran plot for homolog model of 3A4A

According to the Ramachandran plot, 98.1% of residues are found in favored regions while 1.9% of residues are located in allowed regions. Together with no detection of outlier residues, the selected homology model is therefore acceptable. Prior to dock the compounds **31** and **32** with the selected model, the docking parameters were first validated by comparing the conformation Root Mean Square Deviation (RMSD) value of native and re-docked co-crystallized ligand. The parameters are considered successful if the RMSD value is less than 1.5 Å.

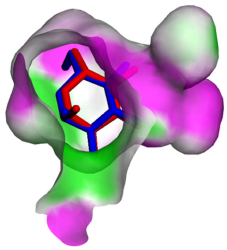

Figure 3. Overlay of re-docked (red) and crystallographic (blue) conformations of alpha-D-glucose in α-glucosidase (3A4A).

As depicted in **Figure 3**, re-docked (red) alpha-D-glucose was found to bind in a similar manner as its respective crystallographic conformations (blue) with the RMSD value of 0.7147 Å, indicating that the selected docking parameters are acceptable. The optimized parameters were then used for the docking of compounds **31** and **32** in the active site of α-glucosidase homology model. **Figure 4** and **Figure 5** illustrated the binding interactions of compounds **31** and **32** in α-glucosidase, respectively.

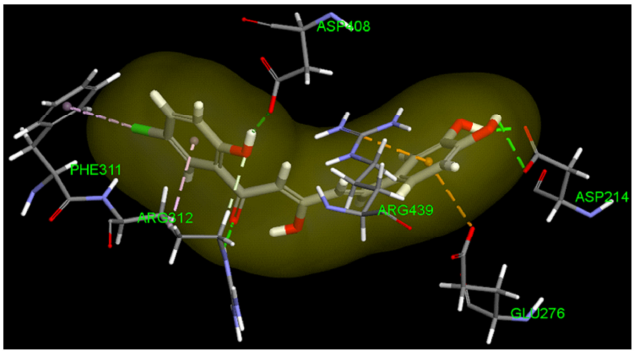

Figure 4. Binding interactions of compound **31** with the active site residues of α-glucosidase receptor

Based on the molecular docking analysis (**Figure 4**), 3,4-dihydroxyphenyl moiety of compound **31** forms two strong hydrogen bonding (green dashed line) interactions with ASP 214 residue. Meanwhile, the phenyl ring of the respective moiety was found to interact with GLU 276 and ARG 439 residues through additional Pi-charge (orange dashed line) interactions. These observations thus explained the critical role of catechol fragment in enhancing the α-glucosidase inhibition. On top of this, both chloro and phenyl moieties of chlrophenol fragment have displayed hydrophobic contacts (light purple dashed line) with PHE 331 and ARG 312 residues at the active site. This could be used to explain the better performance of chlorinated compounds (**29** and **30**) compared to their respective non-chlorinated analogs (**25** and **26**). It is worth noting that the hydroxyl group of chlorophenol fragment and the carbonyl group of pentadienone bridge formed additional hydrogen bonding with ASP 408 and ARG 312 residues, respectively. Ironically, the beneficial effect of chloro moiety was not observed in the comparison of compounds **28** and **31**. This observation may be rationalized with the much higher enhancement degree of catechol moiety which has overshadowed the relatively weaker positive effect of chloro group.

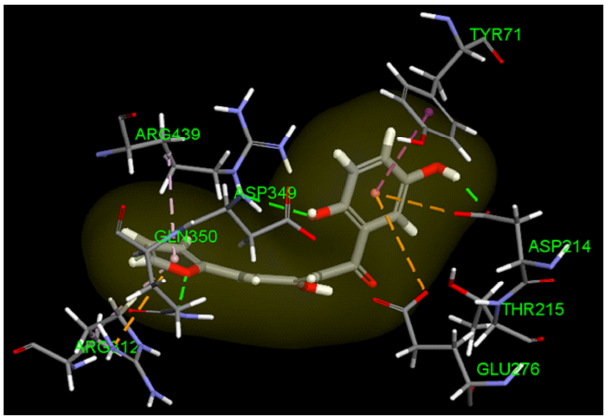

Figure 5. Binding interactions of compound **32** with the active site residues of α-glucosidase receptor

As depicted in **Figure 5**, polyhydroxylated phenyl ring of compound **32** bind in a similar manner as catechol moiety of compound **31**. The *meta*-hydroxy group of compound **32** forms a strong hydrogen bonding with ASP 214. Meanwhile, the respective phenyl ring binds to both ASP 214 and GLU 276 residues with Pi-charge interactions. Apart from ASP 214 and GLU 276 residues, polyhydroxylated phenyl ring of compound **32** is also interacting with TYR 71 and ASP 349 residues through Pi-Pi stacking and hydrogen bonding, respectively. These findings further confirmed the binding mode of polyhydroxyphenyl moiety in α-glucosidase. Interestingly, the furanyl moiety of compound **32** was found to bind with α-glucosidase in a different manner as compared to the chlorophenol ring of compound **31**. The furanyl group forms a Pi-charge interaction with ARG 312 residue. Meanwhile, it also shows hydrophobic contacts with ARG 439 and ARG 312 residues. On top of these, additional hydrogen bonding is also been observed between the oxygen atom of furan ring and GLN 350 residues. The superimpose of compounds **31** and **32** in binding pocket (**Figure 6**) further confirmed the unique role of furanyl moiety as it lays in a small cavity of the active site which failed to be fitted by a phenyl ring. The molecular docking results of compounds **31** and **32** are summarized in **Table 3**.

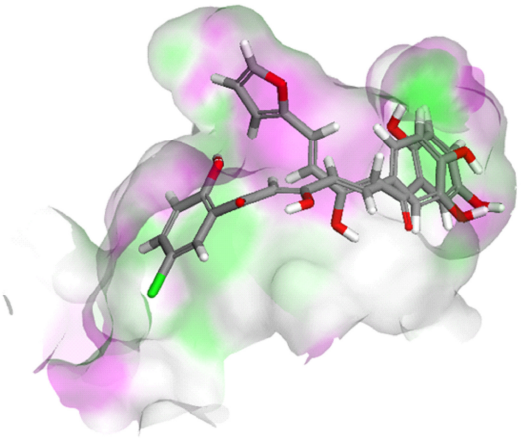

Figure 6. Superimpose of compounds **31** and **32** in binding pocket

Table 3. Data resulted from the molecular docking of compounds **31** and **32** in α-glucosidase.

Compound Structure	Interacting Amino acid residue	Bond type	Bonding distance (Å)
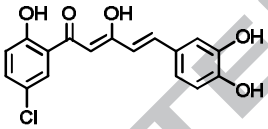 Compound 31	PHE 311	Hydrophobic	5.39
	ARG 312	Hydrophobic	4.23
		Hydrogen bonding	2.03
	ASP 408	Hydrogen bonding	2.00
	ARG 439	Pi-Cation	4.67
	GLU 276	Pi-Anion	4.10
	ASP 214	Hydrogen bonding	1.93, 2.78
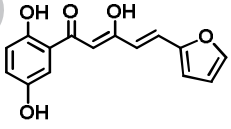 Compound 32	GLN 350	Hydrogen bonding	2.20
	ARG 312	Pi-Cation	4.26
		Hydrophobic	5.19
	ARG 439	Hydrophobic	4.36
		Hydrogen bonding	2.92
	ASP 214	Hydrogen bonding	1.98
		Pi-Anioin	3.70
	THR-2151	Pi-Anioin	4.80
	TYR 71	Pi-Pi stacking	4.85

Taken both *in-vitro* and *in-silico* analyses of diarylpentanoid derivatives on α-glucosidase inhibition, 3,4-dihydroxyphenyl and furanyl rings are the most important functionalities for α-glucosidase inhibitory activity. Since both of them bound to α-glucosidase in a different manner, we therefore concluded that the combination of five membered heterocyclic ring and polyhydroxypheny moiety could be a new lead design in the search of novel α-glucosidase inhibitor.

Acknowledgments

The authors thank the Ministry of Higher Education (MOHE) of Malaysia for financial support under the project FRGS/1/2014/ST01/UPM/02/1 (5538011).

References and notes

1. American Diabetes A. Diagnosis and classification of diabetes mellitus. *Diabetes Care.* **2010**;*33 Suppl 1*: S62-69.
2. Ceriello A. The post-prandial state and cardiovascular disease: relevance to diabetes mellitus. *Diabetes Metab Res Rev.* **2000**;*16*(2): 125-132.
3. Idris I, Thomson GA, Sharma JC. Diabetes mellitus and stroke. *Int J Clin Pract.* **2006**;*60*(1): 48-56.
4. Aoun S, Blacher J, Safar ME, Mourad JJ. Diabetes mellitus and renal failure: effects on large artery stiffness. *J Hum Hypertens.* **2001**;*15*(10): 693-700.
5. Mantovani AM, Fregonesi CE, Palma MR, Ribeiro FE, Fernandes RA, Christofaro DG. Relationship between amputation and risk factors in individuals with diabetes mellitus: A study with Brazilian patients. *Diabetes Metab Syndr.* **2017**;*11*(1): 47-50.
6. Moss SE, Klein R, Klein BE. The incidence of vision loss in a diabetic population. *Ophthalmology.* **1988**;*95*(10): 1340-1348.
7. Takahashi H, Goto T, Shoji T, Tanito M, Park M, Chihara E. Diabetes-associated retinal nerve fiber damage evaluated with scanning laser polarimetry. *Am J Ophthalmol.* **2006**;*142*(1): 88-94.
8. Roglic G, World Health Organization. *Global report on diabetes*. Geneva, Switzerland: World Health Organization; 2016.
9. da Rocha Fernandes J, Ogurtsova K, Linnenkamp U, et al. IDF Diabetes Atlas estimates of 2014 global health expenditures on diabetes. *Diabetes Res Clin Pract.* **2016**;*117*: 48-54.
10. Derosa G, Maffioli P. alpha-Glucosidase inhibitors and their use in clinical practice. *Arch Med Sci.* **2012**;*8*(5): 899-906.
11. Bischoff H. The mechanism of alpha-glucosidase inhibition in the management of diabetes. *Clin Invest Med.* **1995**;*18*(4): 303-311.
12. van de Laar FA. Alpha-glucosidase inhibitors in the early treatment of type 2 diabetes. *Vasc Health Risk Manag.* **2008**;*4*(6): 1189-1195.
13. Lee MY, Choi DS, Lee MK, et al. Comparison of acarbose and voglibose in diabetes patients who are inadequately controlled with basal insulin treatment: randomized, parallel, open-label, active-controlled study. *J Korean Med Sci.* **2014**;*29*(1): 90-97.
14. Shibata E, Aoki K, Tajima K, Taguri M, Terauchi Y. Comparison of efficacy and safety of taking miglitol dissolved in water during a meal and taking a miglitol tablet just before a meal in patients with type 2 diabetes. *Expert Opin Pharmacother.* **2016**;*17*(7): 889-894.
15. Li Q, Chen J, Luo S, Xu J, Huang Q, Liu T. Synthesis and assessment of the antioxidant and antitumor properties of asymmetric curcumin analogues. *Eur J Med Chem.* **2015**;*93*: 461-469.
16. Zhang Y, Zhao C, He W, et al. Discovery and evaluation of asymmetrical monocarbonyl analogs of curcumin as anti-inflammatory agents. *Drug Des Devel Ther.* **2014**;*8*: 373-382.
17. Feng J, Xiao B, Chen W, et al. Synthesis and Anti-Inflammatory Evaluation of Novel C66 Analogs for the Treatment of LPS-Induced Acute Lung Injury. *Chem Biol Drug Des.* **2015**;*86*(4): 753-763.
18. Qiu C, Hu Y, Wu K, et al. Synthesis and biological evaluation of allylated mono-carbonyl analogues of curcumin (MACs) as anti-cancer agents for cholangiocarcinoma. *Bioorg Med Chem Lett.* **2016**;*26*(24): 5971-5976.
19. Manohar S, Khan SI, Kandi SK, et al. Synthesis, antimalarial activity and cytotoxic potential of new monocarbonyl analogues of curcumin. *Bioorg Med Chem Lett.* **2013**;*23*(1): 112-116.
20. Sanabria-Rios DJ, Rivera-Torres Y, Rosario J, et al. Synthesis of novel C5-curcuminoid-fatty acid conjugates and mechanistic investigation of their anticancer activity. *Bioorg Med Chem Lett.* **2015**;*25*(10): 2174-2180.
21. Wang R, Chen C, Zhang X, et al. Structure-Activity Relationship and Pharmacokinetic Studies of 1,5-Diheteroarylpenta-1,4-dien-3-ones: A Class of Promising Curcumin-Based Anticancer Agents. *J Med Chem.* **2015**;*58*(11): 4713-4726.
22. Velaithan V, Okuda KS, Ng MF, et al. Zebrafish phenotypic screen identifies novel Notch antagonists. *Invest New Drugs.* **2017**;*35*(2): 166-179.
23. Liu Z, Sun Y, Ren L, et al. Evaluation of a curcumin analog as an anti-cancer agent inducing ER stress-mediated apoptosis in non-small cell lung cancer cells. *BMC Cancer.* **2013**;*13*: 494.
24. Yuan X, Li H, Bai H, et al. Synthesis of novel curcumin analogues for inhibition of 11beta-hydroxysteroid dehydrogenase type 1 with anti-diabetic properties. *Eur J Med Chem.* **2014**;*77*: 223-230.
25. Wang Y, Yu C, Pan Y, et al. A novel synthetic monocarbonyl analogue of curcumin, A13, exhibits anti-inflammatory effects in vivo by inhibition of inflammatory mediators. *Inflammation.* **2012**;*35*(2): 594-604.
26. Leong SW, Faudzi SMM, Abas F, et al. Synthesis and sar study of diarylpentanoid analogues as new anti-inflammatory agents. *Molecules.* **2014**;*19*(10): 16058-16081.
27. Faudzi SM, Leong S, Abas F, et al. Synthesis, biological evaluation and QSAR studies of diarylpentanoid analogues as potential nitric oxide inhibitors. *MedChemComm.* **2015**;*6*(6): 1069-1080.
28. Leong SW, Mohd Faudzi SM, Abas F, et al. Nitric oxide inhibitory activity and antioxidant evaluations of 2-benzoyl-6-benzylidenecyclohexanone analogs, a novel series of curcuminoid and diarylpentanoid derivatives. *Bioorg Med Chem Lett.* **2015**;*25*(16): 3330-3337.
29. Mohd Aluwi MF, Rullah K, Yamin BM, et al. Synthesis of unsymmetrical monocarbonyl curcumin analogues with potent inhibition on prostaglandin E2 production in LPS-induced murine and human macrophages cell lines. *Bioorg Med Chem Lett.* **2016**;*26*(10): 2531-2538.
30. Leong SW, Faudzi SM, Abas F, et al. Synthesis and sar study of diarylpentanoid analogues as new anti-

inflammatory agents. *Molecules.* **2014**;*19*(10): 16058-16081.

31. *General procedure for synthesis of I and II.* A catalytic amount of *p*-toluenesulphonic acid was added into a mixture of cyclohexanone (20 mmol) and pyrrolidine (20 mmol) in 30 mL of toluene kept in 100 mL SNRB at room temperature. The mixture was then refluxed on a Dean & Stark apparatus for 2 hours to prepare **I**. Upon completion, 20 mmol of benzaldehyde in 20 mL of toluene was added dropwise into the reaction solution (**I**) and heat at 80˚C for 8 hours. Distilled water (10 ml) was then added and further refluxed for 30 min. The resulting reaction mixture was extracted thrice with 3M HCl and once with 20 mL water. The toluene layer was dried over anhydrous magnesium sulphate and concentrated in vacuo to give **II**, 2-benzylidenecyclohexanone. The resulting crude product was purified by column chromatography.

General procedure for the synthesis of III (pathway d). In a 50 mL SNRB, 2-benzylidenecyclohexanone (5 mmol) and appropriate aromatic aldehyde (5 mmol) were dissolved in 30 mL of absolute ethanol. Catalytic amount of 6M NaOH solution was added and the reaction mixture was stirred for overnight. The resulting mixture was then neutralized with 3M HCl followed by extraction with EA. The organic layer was then dried over anhydrous magnesium sulphate and evaporated using rotatory evaporator. The target compound was purified by gravitational column chromatography.

General procedure for the synthesis of III (pathway e). In a 50 mL SNRB, 2-benzylidenecyclohexanone (5 mmol) and appropriate aromatic aldehyde (5 mmol) were dissolved in 30 mL of acetic acid. Catalytic amount of concentrated sulfuric acid was added and reaction mixture was stirred for overnight. The resulting mixture was extracted with EA and washed with 10% sodium bicarbonate solution. The organic layer was then dried over anhydrous magnesium sulphate and evaporated using rotatory evaporator. The target compound was purified by gravitational column chromatography.

2-Benzylidene-6-(2-fluorobenzylidene)cyclohexanone (***1***). Yellow; m.p.: 90-92ºC; Mass calculated: 292.1263; Mass found: 292.1274. ^{1}H NMR (500 MHz, $CDCl_3$) δ:1.78 (dt, *J*=12.72, 6.36 Hz, 2 H) 2.78 - 2.83 (m, 2 H) 2.91 - 2.96 (m, 2 H) 7.08 - 7.14 (m, 1 H) 7.14 - 7.19 (m, 1 H) 7.29 - 7.38 (m, 3 H) 7.39 - 7.43 (m, 2 H) 7.45 - 7.49 (m, 2 H) 7.81 (s, 1 H) 7.83 (s, 1 H). ^{13}C NMR (126 MHz, $CDCl_3$) δ: 23.0, 28.4, 28.6, 115.8, 123.7, 128.4, 128.7, 129.4, 130.3, 130.4, 130.7, 135.9, 136.0, 137.4, 161.6, 163.6, 190.0

2-Benzylidene-6-(3-fluorobenzylidene)cyclohexanone (***2***). Yellow; m.p.: 92-93ºC; Mass calculated: 292.1263; Mass found: 292.1287. ^{1}H NMR (500 MHz, $CDCl_3$) δ: 1.80 (quin, *J*=6.36 Hz, 2 H) 2.87 - 2.98 (m, 4 H) 7.01 - 7.07 (m, 1 H) 7.16 (d, *J*=10.40 Hz, 1 H) 7.23 (d, *J*=7.51 Hz, 1 H) 7.32 - 7.38 (m, 2 H) 7.41 (t, *J*=7.51 Hz, 2 H) 7.44 - 7.49 (m, 2 H) 7.73 (s, 1 H) 7.81 (s, 1 H). ^{13}C NMR (126 MHz, $CDCl_3$) δ: 22.9, 28.4, 115.5, 116.7, 126.2, 126.2, 128.4, 128.7, 129.8, 129.9, 130.4, 135.4, 135.8, 135.9, 137.2, 137.3, 138.1, 161.6, 163.5, 190.2

2-Benzylidene-6-(4-fluorobenzylidene)cyclohexanone (***3***). Yellow; m.p.: 109-110ºC; Mass calculated: 292.1263; Mass found: 292.1281. ^{1}H NMR (500 MHz, $CDCl_3$) δ: 1.80 (quin, *J*=6.36 Hz, 2 H) 2.87 - 2.97 (m, 4 H) 7.10 (t, *J*=8.67 Hz, 2 H) 7.32 - 7.36 (m, 1 H) 7.41 (t, *J*=7.51 Hz, 2 H) 7.43 - 7.48 (m, 4 H) 7.76 (s, 1 H) 7.80 (s, 1 H). ^{13}C NMR (126 MHz, $CDCl_3$) δ: 23.0, 28.4, 28.4, 115.6, 128.4, 128.6, 130.4, 132.2, 132.3, 135.8, 135.9, 136.0, 137.0, 161.6, 163.61, 190.2

2-Benzylidene-6-(3,4-difluorobenzylidene)cyclohexanone (***4***). Yellow; m.p.: 80-81ºC; Mass calculated: 310.1169; Mass found: 310.1178. ^{1}H NMR (500 MHz, $CDCl_3$) δ: 1.81 (quin, *J*=6.21 Hz, 2 H) 2.88 (t, *J*=5.49 Hz, 2 H) 2.94 (t, *J*=5.49 Hz, 2 H) 7.17 - 7.21 (m, 2 H) 7.26 - 7.31 (m, 1 H) 7.32 - 7.37 (m, 1 H) 7.41 (t, *J*=7.51 Hz, 2 H) 7.45 - 7.48 (m, 2 H) 7.67 (s, 1 H) 7.80 (s, 1 H). ^{13}C NMR (126 MHz, $CDCl_3$) δ: 22.8, 28.3, 28.3, 117.4, 118.9, 127.0, 128.4, 128.8, 130.4, 132.9, 134.5, 135.8, 135.8, 136.8, 137.4, 149.3, 151.2, 190.0

2-Benzylidene-6-(2-chlorobenzylidene)cyclohexanone (***5***). Yellow; m.p.: 53-55ºC; Mass calculated: 308.0968; Mass found: 308.0986. ^{1}H NMR (500 MHz, $CDCl_3$) δ: 1.78 (dt, *J*=12.28, 6.29 Hz, 2 H) 2.74 - 2.79 (m, 2 H) 2.92 - 2.96 (m, 2 H) 7.25 - 7.30 (m, 2 H) 7.31 - 7.36 (m, 2 H) 7.38 - 7.49 (m, 5 H) 7.82 (s, 1 H) 7.89 (s, 1 H). ^{13}C NMR (126 MHz, $CDCl_3$) δ: 23.1, 28.2, 28.6, 110.0, 126.2, 128.4, 128.7, 129.5, 129.7, 130.4, 130.5, 133.6, 134.5, 135.0, 136.0, 137.58, 137.9, 190.1

2-Benzylidene-6-(4-chlorobenzylidene)cyclohexanone (***6***). Yellow; m.p.: 105-107ºC; Mass calculated: 308.0968; Mass found: 308.0979. ^{1}H NMR (500 MHz, $CDCl_3$) δ: 1.79 (quin, *J*=6.21 Hz, 2 H) 2.86 - 2.91 (m, 2 H) 2.91 - 2.96 (m, 2 H) 7.32 - 7.43 (m, 7 H) 7.44 - 7.48 (m, 2 H) 7.73 (s, 1 H) 7.80 (s, 1 H). ^{13}C NMR (126 MHz, $CDCl_3$) δ: 22.9, 28.4, 28.5, 128.4, 128.65, 128.69, 130.39, 131.58, 134.37, 134.50, 135.5, 135.9, 136.0, 136.6, 137.2, 142.4, 145.0, 190.1

2-Benzylidene-6-(2,3-dichlorobenzylidene)cyclohexanone (***7***). Yellow; m.p.: 94-95ºC; Mass calculated: 342.0578; Mass found: 342.0591. ^{1}H NMR (500 MHz, $CDCl_3$) δ: 1.77 (dt, *J*=12.72, 6.36 Hz, 2 H) 2.72 (t, *J*=5.20 Hz, 1 H) 2.94 (t, *J*=5.20 Hz, 2 H) 7.19 - 7.24 (m, 2 H) 7.32 - 7.38 (m, 1 H) 7.38 - 7.45 (m, 3 H) 7.45 - 7.49 (m, 2 H) 7.83 (d, *J*=2.31 Hz, 2 H). ^{13}C NMR (126 MHz, $CDCl_3$) δ: 23.0, 28.1, 28.6, 126.8, 128.4, 128.6, 128.8, 130.0, 130.5, 133.3, 133.5, 135.8, 135.8, 137.9, 138.5, 189.9

2-Benzylidene-6-(3,4-dichlorobenzylidene)cyclohexanone (***8***). Yellow; m.p.: 85-86ºC; Mass calculated: 342.0578; Mass found: 342.0583. ^{1}H NMR (500 MHz, $CDCl_3$) δ: 1.80 (dt, *J*=12.28, 6.29 Hz, 2 H) 2.85 - 2.90 (m, 2 H) 2.91 - 2.97 (m, 2 H) 7.25 - 7.29 (m, 1 H) 7.32 - 7.37 (m, 1 H) 7.41 (t, *J*=7.51 Hz, 2 H) 7.44 - 7.49 (m, 3 H) 7.53 (s, 1 H) 7.65 (s, 1 H) 7.80 (s, 1 H). ^{13}C NMR (126 MHz, $CDCl_3$) δ: 22.8, 28.3, 28.4, 128.4, 128.8, 129.5, 130.4, 130.4, 130.9, 131.7, 132.5, 132.6, 134.1, 135.7, 135.9, 137.6, 189.9

2-Benzylidene-6-(2-bromobenzylidene)cyclohexanone (***9***). Orange gummy solid; m.p.: -; Mass calculated: 352.0463; Mass found: 352.0468. ^{1}H NMR (500 MHz, $CDCl_3$) δ: 1.78 (dt, *J*=12.28, 6.29 Hz, 2 H) 2.72 - 2.78 (m, 2 H) 2.90 - 2.96 (m, 2 H) 7.16 - 7.21 (m, 1 H) 7.29 - 7.36 (m, 3 H) 7.39 - 7.43 (m, 2 H) 7.45 - 7.49 (m, 2 H) 7.61 - 7.66 (m, 1 H) 7.83 (s, 2 H). ^{13}C NMR (126 MHz, $CDCl_3$) δ: 23.11, 28.1, 28.6, 107.1, 126.9, 128.4, 128.7, 129.6, 129.8, 130.4, 130.5, 132.9, 133.7, 135.1, 135.9, 135.9, 136.0, 137.6, 190.1

2-benzylidene-6-(3-bromobenzylidene)cyclohexanone (***10***). Yellow; m.p.: 108-109ºC; Mass calculated: 352.0463; Mass found: 352.0475. ^{1}H NMR (500 MHz, $CDCl_3$) δ: 1.80 (quin, *J*=6.21 Hz, 2 H) 2.87 - 2.91 (m, 2 H) 2.92 - 2.96 (m, 2 H) 7.27 (m, *J*=7.51 Hz, 1 H) 7.33 - 7.38 (m, 2 H) 7.39 - 7.43 (m, 2 H) 7.44 - 7.49 (m, 3 H) 7.59 (s, 1 H) 7.70 (s, 1 H) 7.80 (s, 1 H). ^{13}C NMR (126 MHz, $CDCl_3$) δ: 22.9, 28.4, 28.4, 128.4, 128.7, 128.9, 129.9, 130.4, 131.4, 132.8, 135.1, 135.8, 135.9, 137.3, 137.4, 138.0, 190.1

2-Benzylidene-6-(4-bromobenzylidene)cyclohexanone (***11***). Yellow; m.p.: 123-125ºC; Mass calculated: 352.0463; Mass

found: 352.0478. ^{1}H NMR (500 MHz, $CDCl_3$) δ: 1.79 (dt, *J*=12.28, 6.29 Hz, 2 H) 2.85 - 2.90 (m, 2 H) 2.91 - 2.96 (m, 2 H) 7.30 - 7.37 (m, 3 H) 7.41 (t, *J*=7.80 Hz, 2 H) 7.44 - 7.48 (m, 2 H) 7.53 (d, *J*=8.67 Hz, 2 H) 7.71 (s, 1 H) 7.80 (s, 1 H). ^{13}C NMR (126 MHz, $CDCl_3$) δ: 22.9, 28.4, 28.5, 122.8, 128.4, 128.7, 130.4, 131.6, 131.8, 134.8, 135.6, 135.8, 135.9, 136.7, 137.3, 190.2

*2-Benzylidene-6-(3-methylbenzylidene)cyclohexanone (**12**).* Yellow; m.p.: 92-93ºC; Mass calculated: 288.1514; Mass found: 288.1524. ^{1}H NMR (500 MHz, $CDCl_3$) δ: 1.79 (quin, *J*=6.21 Hz, 2 H) 2.39 (s, 3 H) 2.91 - 2.97 (m, 4 H) 7.14 - 7.18 (m, 1 H) 7.25 - 7.37 (m, 4 H) 7.39 - 7.44 (m, 2 H) 7.45 - 7.49 (m, 2 H) 7.78 (s., 1 H) 7.81 (s, 1 H). ^{13}C NMR (126 MHz, $CDCl_3$) δ: 21.5, 23.0, 28.5, 28.5, 127.4, 128.3, 128.4, 128.6, 129.4, 130.4, 131.1, 135.9, 136.0, 136.2, 136.9, 137.1, 137.2, 138.0, 190.4

*2-Benzylidene-6-(4-methylbenzylidene)cyclohexanone (**13**).* Yellow; m.p.: 93-95ºC; Mass calculated: 288.1514; Mass found: 288.1527. ^{1}H NMR (500 MHz, $CDCl_3$) δ: 1.75 - 1.84 (m, 2 H) 2.39 (s, 3 H) 2.93 (td, *J*=6.21, 3.18 Hz, 4 H) 7.22 (d, *J*=8.09 Hz, 2 H) 7.31 - 7.36 (m, 1 H) 7.37 - 7.43 (m, 4 H) 7.45 - 7.49 (m, 2 H) 7.79 (s., 1 H) 7.80 (s., 1 H). ^{13}C NMR (126 MHz, $CDCl_3$) δ: 21.4, 23.0, 28.4, 28.6, 128.4, 128.5, 129.2, 130.4, 130.5, 133.1, 135.4, 136.0, 136.3, 136.7, 137.1, 138.9, 190.4

*2-Benzylidene-6-(4-methoxybenzylidene)cyclohexanone (**14**).* Yellow; m.p.: 96-97ºC; Mass calculated: 304.1463; Mass found: 304.1477. ^{1}H NMR (500 MHz, $CDCl_3$) δ: 1.80 (quin, *J*=6.21 Hz, 2 H) 2.89 - 2.95 (m, 4 H) 3.85 (s, 3 H) 6.92 - 6.96 (m, 2 H) 7.31 - 7.36 (m, 1 H) 7.38 - 7.42 (m, 2 H) 7.44 - 7.48 (m, 4 H) 7.78 (s, 1 H) 7.80 (s, 1 H). ^{13}C NMR (126 MHz, $CDCl_3$) δ: 23.0, 28.4, 28.6, 55.3, 113.9, 128.4, 128.5, 128.6, 130.3, 132.3, 134.1, 136.1, 136.3, 136.5, 137.0, 160.0, 190.3

*2-Benzylidene-6-(2,3-dimethoxybenzylidene)cyclohexanone (**15**).* Yellow gummy solid; m.p.: -; Mass calculated: 334.1569; Mass found: 334.1577. ^{1}H NMR (500 MHz, $CDCl_3$) δ: 1.76 (quin, *J*=6.36 Hz, 2 H) 2.77 - 2.84 (m, 2 H) 2.89 - 2.95 (m, 2 H) 3.82 (s, 3 H) 3.88 (s, 3 H) 6.93 (dd, *J*=7.80, 3.18 Hz, 2 H) 7.04 - 7.09 (m, 1 H) 7.32 - 7.37 (m, 2 H) 7.40 (t, *J*=7.51 Hz, 2 H) 7.45 - 7.48 (m, 2 H) 7.80 (s, 1 H) 7.93 (s, 1 H). ^{13}C NMR (126 MHz, $CDCl_3$) δ: 23.2, 28.5, 28.7, 55.8, 61.2, 112.7, 122.1, 123.5, 128.4, 128.6, 130.4, 132.4, 136.0, 136.3, 137.1, 137.5, 148.3, 159.5, 161.1, 190.0

*2-Benzylidene-6-(2,4-dimethoxybenzylidene)cyclohexanone (**16**).* Yellow; m.p.: 84-86ºC; Mass calculated: 334.1569; Mass found: 334.1579. ^{1}H NMR (500 MHz, $CDCl_3$) δ: 1.77 (quin, *J*=6.21 Hz, 2 H) 2.82 - 2.87 (m, 2 H) 2.89 - 2.94 (m, 2 H) 3.84 (s, 5 H) 6.48 (d, *J*=2.31 Hz, 1 H) 6.51 (dd, *J*=8.38, 2.60 Hz, 1 H) 7.28 - 7.34 (m, 3 H) 7.39 (t, *J*=7.51 Hz, 2 H) 7.43 - 7.47 (m, 2 H) 7.79 (s, 1 H) 8.01 (s, 1 H). ^{13}C NMR (126 MHz, $CDCl_3$) δ: 23.3, 28.6, 28.8, 55.4, 55.5, 98.2, 104.1, 117.9, 128.3, 128.4, 130.3, 131.3, 132.4, 134.5, 136.2, 136.4, 136.6, 160.0, 161.7, 190.4

*2-Benzylidene-6-(2,5-dimethoxybenzylidene)cyclohexanone (**17**).* Yellow gummy solid; Mass calculated: 334.1569; Mass found: 334.1584. ^{1}H NMR (500 MHz, $CDCl_3$) δ: 1.77 (dt, *J*=12.72, 6.36 Hz, 2 H) 2.83 - 2.88 (m, 2 H) 2.90 - 2.95 (m, 2 H) 3.79 (s, 3 H) 3.82 (s, 3 H) 6.82 - 6.90 (m, 3 H) 7.31 - 7.35 (m, 1 H) 7.40 (t, *J*=7.51 Hz, 2 H) 7.44 - 7.48 (m, 2 H) 7.79 (s, 1 H) 7.96 (s, 1 H). ^{13}C NMR (126 MHz, $CDCl_3$) δ: 23.2, 28.5, 28.6, 55.8, 56.1, 110.0, 111.5, 114.5, 116.3, 125.7, 128.3, 128.5, 130.4, 132.4, 136.1, 136.3, 136.6, 136.9, 152.8, 190.4

*2-Benzylidene-6-(3,4,5-trimethoxybenzylidene)cyclohexanone (**18**).* Yellow; m.p.: 105-107ºC; Mass calculated: 364.1675; Mass found: 364.1687. ^{1}H NMR (500 MHz, $CDCl_3$) δ: 1.80 (dt, *J*=12.72, 6.36 Hz, 2 H) 2.89 - 2.98 (m, 4 H) 3.86 - 3.90 (m, 9 H) 6.71 (s, 2 H) 7.31 - 7.36 (m, 1 H) 7.37 - 7.43 (m, 2 H) 7.44 - 7.48 (m, 2 H) 7.72 (s., 1 H) 7.79 (s., 1 H). ^{13}C NMR (126 MHz, $CDCl_3$) δ: 23.0, 28.4, 28.5, 56.2, 61.0, 107.8, 110.0, 128.4, 128.6, 130.4, 131.4, 135.5, 135.9, 136.1, 137.0, 137.2, 152.9, 190.3

*2-Benzylidene-6-(3-hydroxybenzylidene)cyclohexanone (**19**).* Yellow; m.p.: 150-151ºC; Mass calculated: 290.1307; Mass found: 290.1319. ^{1}H NMR (500 MHz, acetone-d_6) δ: 1.79 (quin, J=6.36 Hz, 2 H) 2.93 - 2.97 (m, 4 H) 6.85 - 6.89 (m, 1 H) 6.99 - 7.04 (m, 2 H) 7.25 - 7.31 (m, 1 H) 7.35 - 7.40 (m, 1 H) 7.43 - 7.49 (m, 2 H) 7.51 - 7.56 (m, 2 H) 7.63 (s, 1 H) 7.70 (s, 1 H) 8.56 (br. s., 1 H). ^{13}C NMR (126 MHz, acetone-d_6) δ: 22.8, 28.2, 28.3, 115.8, 116.8, 121.7, 128.4, 128.5, 129.5, 130.3, 135.7, 135.9, 136.0, 136.4, 136.5, 137.3, 157.4, 188.7

*2-Benzylidene-6-(4-hydroxybenzylidene)cyclohexanone (**20**).* Yellow; m.p.: 208-210ºC; Mass calculated: 290.1307; Mass found: 290.1331. ^{1}H NMR (500 MHz, DMSO-d_6) δ: 1.68 (dt, J=12.28, 6.29 Hz, 2 H) 2.84 (t, J=6.65 Hz, 4 H) 6.84 (d, J=8.67 Hz, 2 H) 7.33 - 7.38 (m, 1 H) 7.38 - 7.45 (m, 4 H) 7.46 - 7.52 (m, 2 H) 7.56 (s., 1 H) 7.59 (s., 1 H) 9.96 (br. s., 1 H). ^{13}C NMR (126 MHz, DMSO-d_6) δ: 22.9, 28.2, 28.5, 110.0, 116.0, 126.8, 129.0, 129.1, 130.6, 133.1, 133.5, 135.5, 135.9, 136.9, 137.0, 158.9, 189.1

*2-Benzylidene-6-(3,4-dihydroxybenzylidene)cyclohexanone (**21**).* Yellow; m.p.: 172-174ºC; Mass calculated: 306.1256; Mass found: 306.1271. ^{1}H NMR (500 MHz, acetone-d_6) δ: 1.79 (quin, *J*=6.26 Hz, 2 H) 2.90 - 2.96 (m, 4 H) 6.89 - 6.93 (m, 1 H) 6.98 (dd, *J*=7.93, 1.83 Hz, 1 H) 7.10 (d, *J*=1.83 Hz, 1 H) 7.34 - 7.39 (m, 1 H) 7.45 (t, *J*=7.63 Hz, 2 H) 7.49 - 7.54 (m, 2 H) 7.60 (s, 1 H) 7.68 (s, 1 H) 8.33 (br. s, 2 H). ^{13}C NMR (126 MHz, acetone-d_6) δ: 28.1, 33.3, 33.7, 120.5, 122.6, 122.7, 129.0, 133.3, 133.6, 135.4, 138.8, 140.3, 141.3, 141.9, 150.1, 151.6, 193.7

32. *α-Glucosidase inhibitory assay.* Briefly, 130 µL of sodium phosphate buffer (0.03 M, pH 7.4) was first added to 96-well microplate followed by the addition of 10 µL of α-glucosidase solution and 10 µL of test compounds. The mixture was incubated at 37˚C for 5 min. Then, 50 µL of substrate (4-Nitrophenyl-α-D-glucopyranoside) was added to initiate the enzyme reaction and the reaction mixture was further incubated for 15 min at 37˚C. The reaction was terminated by adding 50 µL of 2M glycine (pH 10) solution. The absorbance of the colored end-product was measured at 405 nm using SpectraMax Plus 384 Microplate Reader (Molecular Devices LLC, Sunnyvale, CA, USA). The final concentrations of α-glucosidase enzyme and DMSO are 0.02 U/well and 0.1 %, respectively. All reactions were carried out in triplicate. The IC_{50} values were calculated in µM using Graph Pad software

33. *General procedure for synthesis of IV.* A catalytic amount of *p*-toluenesulphonic acid was added into a mixture of cyclohexanone (20 mmol) and pyrrolidine (20 mmol) in 30 mL of toluene kept in 100 mL SNRB at room temperature. The mixture was then refluxed on a Dean & Stark apparatus for 2 hours to prepare **I**. Upon completion, 20 mmol of benzoic anhydride in 20 mL of toluene was added dropwise into the reaction solution (**I**) and stirred at room temperature for overnight. Distilled water (10 ml) was then added and further refluxed for 30 min. The resulting reaction mixture was extracted thrice with 3M HCl and

once with 20 mL water. The toluene layer was dried over anhydrous magnesium sulphate and concentrated in vacuo to give **IV**, 2-benzoylcyclohexanone. The resulting crude product was purified by column chromatography.

General procedure for synthesis of V. In a 50 mL SNRB, 2-benzoylcyclohexanone (5 mmol) and appropriate aromatic aldehyde (5 mmol) were dissolved in 30 mL of acetic acid. A catalytic amount of concentrated sulfuric acid was added and the reaction mixture was stirred for overnight. The resulting mixture was extracted with EA and washed with 10% sodium bicarbonate solution. The organic layer was then dried over anhydrous magnesium sulphate and evaporated using rotatory evaporator. The target compound was purified by gravitational column chromatography.

*2-Benzoyl-6-(3-hydroxybenzylidene)cyclohexen-1-ol (**22**).* Yellow; m.p.: 120-121ºC; Mass calculated: 306.1256; Mass found: 306.1258. ^{1}H NMR (500 MHz, $CDCl_3$) δ: 1.66 (quin, J=6.04 Hz, 2 H) 2.53 (t, J=5.97 Hz, 2 H) 2.76 (t, J=5.53 Hz, 2 H) 5.39 (br. s., 1 H) 6.80 (dd, J=8.01, 2.18 Hz, 1 H) 6.91 (s, 1 H) 7.02 (d, J=7.86 Hz, 1 H) 7.22 - 7.29 (m, 1 H) 7.40 - 7.50 (m, 3 H) 7.58 (d, J=7.28 Hz, 2 H) 7.70 (s, 1 H) 16.71 (s, 1 H). ^{13}C NMR (126 MHz, $CDCl_3$) δ: 23.5, 27.2, 27.6, 108.6, 115.4, 116.7, 122.7, 127.6, 128.2, 129.5, 130.7, 132.8, 133.1, 137.8, 138.2, 155.5, 176.2, 195.8

*2-Benzoyl-6-(4-hydroxybenzylidene)cyclohexen-1-ol (**23**).* Yellow; m.p.: 158-160ºC; Mass calculated: 306.1256; Mass found: 306.1268. ^{1}H NMR (500 MHz, $CDCl_3$) δ: 1.68 (quin, J=5.97 Hz, 2 H) 2.53 (t, J=5.82 Hz, 2 H) 2.77 (t, J=5.53 Hz, 2 H) 6.87 (d, J=8.45 Hz, 2 H) 7.38 (d, J=8.15 Hz, 2 H) 7.41 - 7.49 (m, 3 H) 7.57 (d, J=7.28 Hz, 2 H) 7.71 (s, 1 H) 16.87 (s, 1 H). ^{13}C NMR (126 MHz, $CDCl_3$) δ: 23.6, 27.1, 27.7, 108.1, 115.4, 127.6, 128.1, 129.1, 130.5, 130.6, 132.1, 133.4, 138.2, 155.8, 177.5, 194.4

*2-Benzoyl-6-(3,4-dihydroxybenzylidene)cyclohexen-1-ol (**24**).* Yellow; m.p.: 212-213ºC; Mass calculated: 322.1205; Mass found: 322.1215. ^{1}H NMR (500 MHz, acetone-d_6) δ: 1.67 (quin, J=5.61 Hz, 2 H) 2.54 (t, J=5.24 Hz, 2 H) 2.79 (t, J=5.97 Hz, 2 H) 6.87 - 7.00 (m, 2 H) 7.09 (s, 1 H) 7.44 - 7.56 (m, 3 H) 7.58 - 7.68 (m, 3 H) 8.22 (br. s., 2 H) 17.12 (s, 1 H). ^{13}C NMR (126 MHz, acetone-d_6) δ: 23.4, 26.7, 27.5, 107.8, 115.4, 117.2, 123.4, 127.6, 128.1, 128.3, 129.9, 130.5, 133.7, 138.2, 144.9, 146.1, 177.8, 193.8

34. *General procedure for synthesis of VI.* Phosphoryl chloride ($POCl_3$; 20 mmol) was added slowly to a 100 mL SNRB flask containing a mixture of appropriate cinnamic acid (5.5 mmol) and the 2'-hydroxyacetophenone (5 mmol) in ice cooled pyridine (30 mL) and stirred overnight. The reaction mixture was then poured into 100 mL cold, dilute HCl in a 250 mL EF, followed by extraction with ethyl acetate (EA). The organic layer was dried over anhydrous magnesium sulfate and concentrated *in vacuo*. The crude product obtained was further purified by flash chromatography to give cinnamate ester **VI**.

General procedure for synthesis of VII. Purified cinnamate ester **VI** was dissolved with 30 mL of pyridine in 100 mL SNRB flask. Then, ground potassium hydroxide pellets (20 mmol) were added to the solution and stirred overnight at room temperature. Upon completion, the reaction mixture was poured into 150 mL cold, diluted HCl in a 250 mL EF and stirred for 10 min. The solution was extracted with EA and dried over anhydrous magnesium sulfate, followed by solvent removal with rotatory evaporator under *vacuo*. The resulting crude product was further purified by flash chromatography to obtained methoxylated diarylpentanoids. The purified methoxylated diarylpentanoids (0.3 mmol) were then reacted with 1.5 mL boron tribromide (BBr_3) solution in dry dichloromethane (30 mL) at 0 °C. After 8 hours of stirring at room temperature, the reaction mixture was poured into 150 mL of cold water and extracted with EA. The organic layer was collected and dried over anhydrous magnesium sulfate. The resulting crude was finally purified through flash column chromatography to give pure polyhydroxylated compounds **VII**.

*3-Hydroxy-1-(2-hydroxyphenyl)-5-(3-hydroxyphenyl)penta-2,4-dien-1-one (**25**).* Orange; m.p.:149-150ºC; Mass calculated: 282.0892; Mass found: 282.0894. ^{1}H NMR (500 MHz, acetone-d_6) δ: 6.75 (s, 1 H) 6.87 (d, *J*=15.73 Hz, 1 H) 6.91 - 6.94 (m, 1 H) 6.95 - 7.00 (m, 2 H) 7.14 - 7.20 (m, 2 H) 7.25 - 7.31 (m, 1 H) 7.51 - 7.56 (m, 1 H) 7.63 (d, *J*=16.02 Hz, 1 H) 7.94 (dd, *J*=8.30, 1.31 Hz, 1 H) 8.60 (s, 1 H) 12.09 (s, 1 H) 14.64 (br. s., 1 H) ^{13}C NMR (126 MHz, acetone-d_6) δ: 97.3, 114.4, 117.4, 118.3, 119.0, 119.2, 119.7, 122.4, 129.1, 130.0, 136.1, 136.5, 139.8, 157.9, 162.5, 175.1, 196.3.

*3-Hydroxy-1-(2-hydroxyphenyl)-5-(4-hydroxyphenyl)penta-2,4-dien-1-one (**26**).* Orange; m.p.: 149-150ºC; Mass calculated: 282.0892; Mass found: 282.0893. ^{1}H NMR (500 MHz, acetone-d_6) δ: 6.68 (s, 1 H) 6.74 (d, *J*=15.73 Hz, 1 H) 6.89 - 6.99 (m, 4 H) 7.49 - 7.54 (m, 1 H) 7.59 (d, *J*=8.74 Hz, 2 H) 7.66 (d, *J*=16.02 Hz, 1 H) 7.92 (dd, *J*=8.30, 1.31 Hz, 1 H) 9.16 (br. s., 1 H) 12.15 (br. s., 1 H) 14.79 (br. s., 1 H). ^{13}C NMR (126 MHz, acetone-d_6) δ: 97.9, 101.6, 101.6, 121.3, 124.2, 124.3, 131.9, 134.2, 135.3, 141.0, 145.5, 165.1, 167.6, 181.4, 193.2.

*5-(2,4-Dihydroxyphenyl)-3-hydroxy-1-(2-hydroxyphenyl)penta-2,4-dien-1-one (**27**).* Brown; m.p.: 90-92ºC; Mass calculated: 298.0841; Mass found: 298.0845. ^{1}H NMR (500 MHz, acetone-d_6) δ: 6.47 (d, *J*=8.45 Hz, 1 H) 6.51 (s, 1 H) 6.62 (s, 1 H) 6.83 (d, *J*=16.02 Hz, 1 H) 6.92 - 6.97 (m, 2 H) 7.47 - 7.53 (m, 2 H) 7.94 (d, *J*=8.45 Hz, 1 H) 8.00 (d, *J*=16.02 Hz, 1 H) 9.15 (br. s., 2 H) 12.23 (br. s., 1 H) 14.88 (br.s., 1 H). ^{13}C NMR (126 MHz, acetone-d_6) δ: 95.9, 102.8, 108.4, 114.4, 118.2, 118.3, 119.0, 119.1, 128.9, 130.4, 135.5, 136.4, 158.6, 161.1, 162.4, 177.3, 195.2.

*5-(3,4-Dihydroxyphenyl)-3-hydroxy-1-(2-hydroxyphenyl)penta-2,4-dien-1-one (**28**).* Orange; m.p.: 155-156ºC; Mass calculated: 298.0841; Mass found: 298.0843. ^{1}H-NMR (500 MHz, acetone-d_6) δ: 6.65–6.73 (m, 2 H) 6.88–7.00 (m, 3 H) 7.11 (d, *J* = 8.2 Hz, 1 H) 7.23 (s, 1 H) 7.52 (t, *J* = 7.86 Hz, 1 H) 7.61 (d, *J* = 15.73 Hz, 1 H) 7.92 (d, *J* = 8.15 Hz, 1 H) 8.28 (br. s, 1 H) 8.61 (br. s, 1 H) 12.19 (s, 1 H) 14.81 (br. s., 1 H). ^{13}C-NMR (126 MHz, acetone-d_6) δ: 96.4, 114.3, 115.6, 118.3, 119.0, 119.1, 119.1, 121.9, 127.5, 128.9, 135.8, 140.6, 145.6, 148.0, 162.4, 176.2, 195.6.

*1-(5-Chloro-2-hydroxyphenyl)-3-hydroxy-5-(3-hydroxyphenyl)penta-2,4-dien-1-one (**29**).* Yellow; m.p.: 181-182ºC; Mass calculated: 316.0502; Mass found: 316.0504. ^{1}H NMR (500 MHz, acetone-d_6) δ: 6.82 (s, 1 H) 6.87 - 6.95 (m, 2 H) 7.00 (d, *J*=9.03 Hz, 1 H) 7.14 - 7.21 (m, 2 H) 7.25 - 7.32 (m, 1 H) 7.52 (dd, *J*=8.88, 2.48 Hz, 1 H) 7.66 (d, *J*=16.02 Hz, 1 H) 7.94 (d, *J*=2.62 Hz, 1 H) 8.62 (s, 1 H) 12.06 (s, 1 H) 14.57 (br. s., 1 H). ^{13}C NMR (126 MHz, acetone-d_6) δ: 97.4, 114.5, 117.6, 119.7, 120.0, 120.2, 122.2, 123.5, 128.2, 130.1, 135.5, 136.5, 140.5, 157.9, 161.0, 176.0, 194.7.

*1-(5-Chloro-2-hydroxyphenyl)-3-hydroxy-5-(4-hydroxyphenyl)penta-2,4-dien-1-one (**30**).* Yellow; m.p.: 183-184ºC; Mass calculated: 316.0502; Mass found: 316.0506. ^{1}H NMR (500 MHz, acetone-d_6) δ: 6.74 (s, 1 H) 6.77 (d, *J*=16.02 Hz, 1 H) 6.93 (d, *J*=8.74 Hz, 2 H) 6.98 (d,

J=8.74 Hz, 1 H) 7.50 (dd, *J*=9.03, 2.62 Hz, 1 H) 7.60 (d, *J*=8.74 Hz, 2 H) 7.70 (d, *J*=16.02 Hz, 1 H) 7.92 (d, *J*=2.62 Hz, 1 H) 9.04 (s, 1 H) 12.13 (s, 1 H) 14.73 (br. s., 1 H). ^{13}C NMR (126 MHz, acetone-d_6) δ: 96.5, 116.0, 118.8, 120.1, 123.4, 126.7, 128.0, 130.3, 135.2, 140.9, 157.6, 160.0, 160.9, 177.1, 194.0.

*1-(5-Chloro-2-hydroxyphenyl)-5-(3,4-dihydroxyphenyl)-3-hydroxypenta-2,4-dien-1-one (**31**).* Orange; m.p.: 177-178ºC; Mass calculated: 332.0452; Mass found: 332.0462. ^{1}H NMR (500 MHz, acetone-d_6) δ: 6.67 - 6.75 (m, 2 H) 6.91 (d, *J*=8.15 Hz, 1 H) 6.98 (d, *J*=9.03 Hz, 1 H) 7.11 (dd, *J*=8.15, 2.04 Hz, 1 H) 7.22 (d, *J*=2.04 Hz, 1 H) 7.50 (dd, *J*=8.88, 2.48 Hz, 1 H) 7.63 (d, *J*=15.73 Hz, 1 H) 7.92 (d, *J*=2.33 Hz, 1 H) 8.41 (br. s., 2 H) 12.15 (br. s., 1 H) 14.72 (br. s., 1 H). ^{13}C NMR (126 MHz, acetone-d_6) δ: 96.5, 114.4, 115.7, 118.9, 120.1, 120.1, 122.1, 123.4, 127.4, 128.0, 135.2, 141.3, 145.6, 148.2, 160.9, 177.1, 194.0.

*1-(2,5-Dihydroxyphenyl)-5-(furan-2-yl)-3-hydroxypenta-2,4-dien-1-one (**32**).* Brown; m.p.: 142-143ºC; Mass calculated: 272.0685; Mass found: 272.0690. ^{1}H NMR (500 MHz, acetone-d_6) δ: 6.62 - 6.65 (m, 2 H) 6.67 (d, *J*=15.73 Hz, 1 H) 6.83 (d, *J*=8.74 Hz, 1 H) 6.88 (d, *J*=3.20 Hz, 1 H) 7.10 (dd, *J*=8.88, 2.77 Hz, 1 H) 7.34 (d, *J*=2.91 Hz, 1 H) 7.49 (d, *J*=15.73 Hz, 1 H) 7.76 (s, 1 H) 8.15 (s, 1 H) 11.51 (s, 1 H) 14.75 (br. s., 1 H). ^{3}C NMR (126 MHz, acetone-d_6) δ: 97.4, 112.8, 113.5, 115.3, 118.9, 118.9, 119.8, 124.5, 126.1, 145.5, 149.6, 151.7, 155.9, 174.8, 195.7.

*1,5-Bis(2,5-dihydroxyphenyl)-3-hydroxypenta-2,4-dien-1-oneone (**33**).* Orange; m.p.: 195-196ºC; Mass calculated: 314.0790; Mass found: 314.0800. ^{1}H NMR (500 MHz, acetone-d_6) δ: 6.59 (s, 1 H) 6.76 - 6.86 (m, 3 H) 6.91 (d, *J*=16.02 Hz, 1 H) 7.06 - 7.11 (m, 2 H) 7.33 (d, *J*=2.91 Hz, 1 H) 7.97 (br. s., 1 H) 8.01 (d, *J*=16.02 Hz, 1 H) 8.13 (br. s., 1 H) 8.58 (br. s., 1 H) 11.55 (s, 1 H) 14.85 (br. s., 1 H). ^{13}C NMR (126 MHz, acetone-d_6) δ: 97.0, 113.4, 113.4, 117.0, 118.9, 118.9, 119.0, 121.7, 122.4, 124.3, 135.4, 149.5, 150.0, 150.6, 155.8, 181.8, 195.6.

*1-(2,4-Dihydroxyphenyl)-5-(2,5-dihydroxyphenyl)-3-hydroxypenta-2,4-dien-1-one (**34**).* Orange; m.p.: 190-191ºC; Mass calculated: 314.0790; Mass found: 314.0792. ^{1}H NMR (500 MHz, acetone-d_6) δ: 6.34 - 6.38 (m, 1 H) 6.46 (dd, *J*=8.88, 2.18 Hz, 1 H) 6.53 (s, 1 H) 6.76 - 6.80 (m, 1 H) 6.81 - 6.88 (m, 2 H) 7.08 (d, *J*=2.62 Hz, 1 H) 7.83 (d, *J*=8.74 Hz, 1 H) 7.93 (d, *J*=16.02 Hz, 1 H) 8.62 (br. s., 3 H) 12.56 (br. s., 1 H) 14.47 (br. s., 1 H). ^{13}C NMR (126 MHz, acetone-d_6) δ: 96.5, 103.2, 108.3, 112.1, 113.4, 117.0, 118.7, 122.0, 122.6, 131.3, 134.5, 149.9, 150.6, 164.7, 165.4, 174.2, 194.8.

35. *Molecular modeling.* Molecular docking studies were carried out using Discovery Studio 3.1 (Accelrys, San Diego, USA) on an Intel® (TM)2 Quad CPU Q8200 @2.33 GHz running under a Windows XP Professional environment.

Homology modeling. The crystal structure of isomaltase (PDB: 3A4A) from Saccharomyces cerevisiae and α-glucosidase sequence (P53341) of Saccharomyces cerevisiae were obtained from the Protein Data Bank and UniProt (www.uniprot.org), respectively. Sequence alignment of P53341 on 3A4A was performed using the Discover Studio 3.1. Then, homology models of α-glucosidase was built based on the sequenced template. The homology models built were then validated by Modeler program in Discover Studio 3.1. The model with the lowest modeler objective function was finally selected for ramachandran plot validation prior to molecular docking.

Ligands preparation. Compounds **35** and **36**, as well as co-crystallized ligands (alpha-D-glucose) were drawn with ChemDraw Ultra 12.0. Then, the structures were imported to the Discovery Studio 3.1 followed by ligands preparation protocol with the default setting, as recommended by Accelrys. The prepared ligands were then subjected to ligands minimization with CHARMm force field before being used for docking analyses

Flexible docking. Minimized co-crystallized ligands were re-docked into their respective enzymes with several sets of amino acids as flexible residues. The top-ranked conformations resulted from the docking experiment were compared to their original crystallographic confirmation in terms of RMSD. The parameters with lowest RMSD values were selected for the flexible docking of compounds **35** and **36** in the homology model. The flexible docking results were analyzed using Discovery Studio Visualizer v4.1.0.14169 (Accelrys, San Diego, USA).

36. Lovell SC, Davis IW, Arendall WB, 3rd, et al. Structure validation by Calpha geometry: phi,psi and Cbeta deviation. *Proteins.* **2003**;*50*(3): 437-450.